


*Editors*  
*Genadiy Pivnyak*  
*Volodymyr Bondarenko*  
*Iryna Kovalevs'ka*  
*Mykhaylo Illiashov*



**Annual Scientific-Technical Collection**

# MINING OF MINERAL DEPOSITS

 **CRC Press**  
Taylor & Francis Group  
A BALKEMA BOOK

**2013**

# MINING OF MINERAL DEPOSITS



# Taylor & Francis

Taylor & Francis Group

<http://taylorandfrancis.com>

# Mining of Mineral Deposits

*Editors*

**Genadiy Pivnyak**

*Rector of National Mining University, Ukraine*

**Volodymyr Bondarenko**

*Department of Underground Mining, National Mining University, Ukraine*

**Iryna Kovalevs'ka**

*Department of Underground Mining, National Mining University, Ukraine*

**Mykhaylo Illiashov**

*PJSC "Donetsksteel", Ukraine*



**CRC Press**

Taylor & Francis Group

Boca Raton London New York Leiden

---

CRC Press is an imprint of the  
Taylor & Francis Group, an **informa** business

**A BALKEMA BOOK**

*CRC Press/Balkema is an imprint of the Taylor & Francis Group, an informa business*

© 2013 Taylor & Francis Group, London, UK

Typeset by Olga Malova & Kostiantyn Ganushevych, Department of Underground Mining, National Mining University, Dnipropetrovs'k, Ukraine

Printed and bound by LizunovPress Ltd, Dnipropetrovs'k, Ukraine

All rights reserved. No part of this publication or the information contained here in may be reproduced, stored in a retrieval system, or transmitted in any form or by any means, electronic, mechanical, by photocopying, recording or otherwise, without written prior permission from the publisher.

Although all care is taken to ensure integrity and the quality of this publication and the information herein, no responsibility is assumed by the publishers nor the author for any damage to the property or persons as a result of operation or use of this publication and/or the information contained herein.

Published by: CRC Press/Balkema

P.O. Box 11320, 2301 EH Leiden, The Netherlands

e-mail: [Pub.NL@taylorandfrancis.com](mailto:Pub.NL@taylorandfrancis.com)

[www.crcpress.com](http://www.crcpress.com) – [www.taylorandfrancis.co.uk](http://www.taylorandfrancis.co.uk) – [www.balkema.nl](http://www.balkema.nl)

ISBN: 978-1-138-00108-4 (Hbk)

ISBN: 978-1-315-86747-2 (eBook)

## Table of contents

Preface	X
New-generation technique and technology for leakage tests <i>A. Bulat, O. Voloshyn, S. Ponomarenko &amp; D. Gubenko</i>	1
Optimal parameters of wall bolts computation in the united bearing system of extraction workings frame-bolt support <i>V. Bondarenko, I. Kovalevs'ka, R. Svystun &amp; Yu. Cherednichenko</i>	5
Pillars sizing at magnetite quartzites room-work <i>N. Stupnik, V. Kalinichenko &amp; S. Pismennyi</i>	11
The calculation scheme of mathematical modeling of displacement process of a terrestrial surface by working out of coal layers <i>M. Antoshchenko, L. Chepurnaya &amp; M. Filatyev</i>	17
Changes of overburden stresses in time and their manifestations in seismic wave indices <i>A. Antsyferov, A. Trifonov, V. Tumanov &amp; L. Ivanov</i>	23
Specifics of percarbonic rock mass displacement in longwalls end areas and extraction workings <i>I. Kovalevs'ka, V. Vivcharenko &amp; V. Snigur</i>	29
Operations under combined method of mining graphite deposit <i>V. Buzylo, T. Savelieva, V. Serduk &amp; T. Morozova</i>	35
Plasma reactor for thermochemical preparation of coal-air mixture before its burning in the furnaces <i>A. Bulat, O. Voloshyn &amp; O. Zhevzhik</i>	39
The influence of fine particles of binding materials on the strength properties of hardening backfill <i>O. Kuz'menko &amp; M. Petlyovanyy &amp; M. Stupnik</i>	45
Magnetite quartzite mining is the future of Kryvyi Rig iron ore basin <i>M. Stupnik &amp; V. Kalinichenko</i>	49
Microalloyed steels for mining supports <i>M. Rotkegel, S. Prusek, R. Kuziak &amp; M. Grodzicki</i>	53
Induction heating in electrotechnology of machine parts dismantling <i>V. Driban, A. Novikov &amp; I. Shestopalov</i>	59
Studies of stationary supporting zone sizes varied in the course of mining operations in deep horizons <i>O. Voloshyn &amp; O. Ryabtsev</i>	71

Influence mechanism of rock mass structure forming a stress on a face support <i>G. Symanovych, M. Demydov &amp; V. Chervatuk</i>	77
Prospects for the bioindication methods implementation in the environmental management system of industrial enterprises <i>A. Gorova A. Pavlychenko &amp; T. Kholodenko</i>	83
Hydrogeodynamics of the contact surface “lining-saturated rocks” in opening mine working <i>I. Sadovenko &amp; V. Tymoshchuk</i>	85
Conditions for minerals extraction from underground mines in the border areas against the seismic and rockburst hazards <i>A. Zorychta, P. Wojtas, A. Mirek &amp; P. Litwa</i>	91
Formation principles of the scientific system of ecological management at the industrial enterprises <i>A. Bardas &amp; O. Parshak</i>	99
Fundamentals of highly loaded coal-water slurries <i>V. Biletskyi, P. Sergejev &amp; O. Krut</i>	105
Genetic classification of gas hydrates deposits types by geologic-structural criteria <i>V. Bondarenko, E. Maksymova &amp; O. Koval</i>	115
The recourse-saving compositions of backfilling mixtures based on slag waste products <i>P. Dolzhikov, S. Syemiryagin &amp; P. Furdey</i>	121
Justification of the gasification channel length in underground gas generator <i>V. Falshtyn's'kyy, R. Dychkovs'kyy, V. Lozyns'kyy &amp; P. Saik</i>	125
Assessment of auger mining application in Polish hard coal deep mines <i>Z. Lubosik</i>	133
The enhancement of hydrocarbon recovery from depleted gas and gas-condensate fields <i>O. Kondrat</i>	143
Study of rock geomechanical processes while mining two-level interchamber pillars <i>V. Russkikh, A. Yavors'kyy, S. Zubko &amp; Ye. Chistyakov</i>	149
Heat pumps for mine water waste heat recovery <i>V. Samusya, Y. Oksen, M. Radiuk</i>	153
Research of stress-strain state of cracked coal-containing massif near-the-working area using finite elements technique <i>I. Kovalevs'ka, G. Symanovych &amp; V. Fomychov</i>	159
The results of instrumental observations on rock pressure in order to substantiate complete excavation of coal reserves <i>Yu. Khalymendyk, A. Bruy &amp; Yu. Zabolotnaya</i>	165

The study of ecological state of waste disposal areas of energy and mining companies <i>A. Gorova, A. Pavlychenko &amp; O. Borysovs'ka</i>	169
The main technical solutions in rational excavation of minerals in open-pit mining <i>M. Chetverik, E. Bubnova &amp; E. Babiy</i>	173
Method of calculation of the minimum pressure of hydro breaking of the coal layer <i>D. Vasilyev, Y. Polyakov &amp; A. Potapenko</i>	177
Main directions and objectives of diversification processes in coal regions of Donbass <i>A. Petenko &amp; E. Nikolaenko</i>	181
Complex use of coal of Northern part of Donbass <i>V. Savchuk, V. Prykhodchenko, V. Buzylo, D. Prykhodchenko &amp; V. Tykhonenko</i>	185
On the limit angles of inclination of belt conveyors <i>V. Monastyr'skiy, R. Kiriya, D. Nomerovs'kiy &amp; N. Larionov</i>	193
Investigation of the rock massif stress strain state in conditions of the drainage drift overworking <i>V. Sotskov &amp; I. Saleev</i>	197
Methodology of gas hydrates formation from gaseous mixtures of various compositions <i>M. Ovchynnikov, K. Ganushevyh &amp; K. Sai</i>	203
The development of methodology for assessment of environmental risk degree in mining regions <i>A. Gorova, A. Pavlychenko, O. Borysovs'ka &amp; L. Krups'ka</i>	207
Bolt support application peculiarities during support of development workings in weakly metamorphosed rocks <i>V. Lapko, V. Fomychov &amp; V. Pochepov</i>	211
Pressure variation of caved rocks in mined-out area of face <i>O. Dotsenko</i>	217
Magnetic stimulation of transformations in coal <i>V. Soboliev, N. Bilan &amp; D. Samovik</i>	221
Receipt of coagulant of water treatment from radio-active elements <i>O. Svetkina</i>	227
Blasting works technology to decrease an emission of harmful matters into the mine atmosphere <i>O. Khomenko, M. Kononenko &amp; I. Myronova</i>	231
The investigation of rock dumps influence to the levels of heavy metals contamination of soil <i>A. Pavlychenko &amp; A. Kovalenko</i>	237



The magnetic susceptibility of granular manganese sludge of Nikopol'sky Basin <i>A. Zubarev</i>	239
Inner potential of technological networks of coal mines <i>S. Salli, O. Mamaykin &amp; S. Smolanov</i>	243
On parameters influence evaluating method application in some geotechnical tasks <i>G. Larionov, R. Kirija &amp; D. Braginec</i>	247
New technical solutions during mining C <sub>5</sub> coal seam under complex hydro-geological conditions of western Donbass <i>V. Russkikh, Yu. Demchenko, S. Salli &amp; O. Shevchenko</i>	257
Effect of degasification efficiency of gas-emission sources under complex degassing on maximum load on a stope as for gas factor <i>O. Mukha, I. Pugach &amp; L. Tokar</i>	261
Modification of cement-loess mixtures in jet technology during mastering underground area <i>S. Vlasov, N. Maksymova-Gulyaeva &amp; E. Maksymova</i>	267
The modernization of ways of treatment of coal stratum for rise of safety of underground mine work <i>V. Pavlysh, O. Grebyonkina, S. Grebyonkin &amp; V. Ryabichev</i>	273
About the influence of stability of workings on the parameters of their ventilation in terms of anthracitic Donbass mines <i>P. Dolzhikov, A. Kipko, N. Paleychuk &amp; Yu. Dolzhikov</i>	277
In-stream settling tank for effective mine water clarification <i>V. Kolesnyk, D. Kulikova &amp; S. Kovrov</i>	285
Rationale of method of unloading area rocks around of developments workings for her repeated use <i>O. Remizov</i>	291
Technological parameters of cutoff curtains, created with the help of inkjet technology <i>O. Vladyko</i>	299
The investigation of coal mines influence on ecological state of surface water bodies <i>A. Gorova, A. Pavlychenko, S. Kulyna &amp; O. Shkremetko</i>	303
Experimental researches of geomechanical characteristics of railway and point switches of underground transport <i>V. Govorukha</i>	307
On the question of implementation prospects of selective mining for exploitation unconditional coal seams <i>D. Astafiev &amp; Y. Shapovalov</i>	313
Study of mechanical half-mask pressure along obturation bar <i>S. Cheberyachko, O. Yavors'ka &amp; T. Morozova</i>	317

Research of mine workings stability on volumetric models made from optically active materials <i>P. Ponomarenko</i>	323
Researches of structural-mechanical properties of coal tailings as disperse systems <i>O. Gayday</i>	327
Theoretical investigation of dry frictional separation of materials on rotating cylinder <i>Yu. Mostyka, V. Shutov, L. Grebenyuk &amp; I. Ahmetshina</i>	333
Influence of undermined terrain mesorelief on accuracy of forecasting subsidence and deformation of earth surface <i>M. Grischenkov &amp; E. Blinnikova</i>	343
Aspects of sulphurous feed extraction in Ukraine <i>V. Kharchenko &amp; O. Dolgyy</i>	347
The stress-strain state of the belt on a drum under compression by flat plates <i>D. Kolosov, O. Dolgov &amp; A. Kolosov</i>	351
Multifactorial mathematical model of mechanical drilling speed <i>M. Moisyshyn, B. Borysevych &amp; R. Shcherbiy</i>	359
Elastic waves influence upon enhancement of shale rocks fracturing <i>Ya. Bazhaluk, O. Karpash, I. Kysil, Ya. Klymyshyn, O. Gutak &amp; Yu. Voloshyn</i>	369

## Preface

The present collection of scientific papers is addressed to mining engineers, scientific and research personnel, students, postgraduates and all professionals connected with the coal and ore industry.

The papers published describe topics related to mine workings drivage, optimization of longwall working parameters, modeling of mine support interaction with rock massif, stress strain state of rock massif during mining operations, geomechanical tasks solving, economic aspects and environment protection.

Additional information is provided regarding recovery and utilization of mine methane, borehole underground coal gasification and alternative energy sources development such as gas hydrates.

Genadiy Pivnyak  
Volodymyr Bondarenko  
Iryna Kovalevs'ka  
Mykhaylo Illiashov

# New-generation technique and technology for leakage tests

A. Bulat, O. Voloshyn & S. Ponomarenko

*M.S. Polyakov Institute of Geotechnical Mechanics, Dnipropetrovs'k, Ukraine*

D. Gubenko

*Yuznoye State Design Office named after M.K. Yangel, Dnipropetrovs'k, Ukraine*

**ABSTRACT:** This article describes principle and mathematic model for testing various devices for leakage with the help of fixed-volume method; shows advantages of this method when compared with manometric methods with no pressure chamber; and presents functional arrangement for applying the method under consideration in industries.

## 1 INTRODUCTION

Energy saving is the key issue of economic development in any country. One of the main types of energy for mineral mining is compressed air which is widely used in the industry thanks to highly safe pneumatic equipment. It is especially important for gassy and dusty mines and, besides, in some cases usage of compressed air is the only possible way when electric power is dangerous to be used for the mineral mining in underground mines under the coal burst and gas release hazard. However, air ducts and pneumatic devices in the active mines are in such condition that requires special measures in order to reduce direct energy inputs and material resources when compressed air is used. Today nonproduction cost of compressed air supplied to the mining equipment is very high, and the problem to cut the cost is a strong business case as tariffs for the energy carrier are growing.

One of the ways to save energy at compressed air production, transportation to and consumption by the mining pneumatic equipment is minimization of the compressed air losses through the improved leak proofness in the pneumatic systems and equipment. With this end in view, the mining companies should improve their standards for testing the pneumatic equipment and air-supply system for leakage in the course of repair and preventive maintenance.

## 2 RESULTS OF THE STUDY

The most widely spread method of testing pneumatic devices with no pressure chamber is manometric method which determines value of the air pressure drop per time unit. This method is known

as pressure drop method. Its main drawback is essential inaccuracy caused by impact of environment parameter gradient on accuracy of the leakage tests. This drawback can be eliminated with the help of fixed-volume method at which:

- two similar vessels (reference vessel and compensating vessel) are used;
- the vessels and device which measures differential pressure between the vessels are located inside the closed thermostat;
- value of factual total leakage in the system or device is determined by the varied gas mass value in the compensating vessel;
- mathematic model which calculates total leakage size takes into account factual variations of gas pressure and temperature in the device under consideration.

Functional arrangement of components for testing device for leakage with the help of the fixed-volume method is shown in the Figure 1.

In this scheme, device 1, which is a compressed-air consumer (volume  $V_1$ ) in the mine, is connected to the compensating vessel 7 and reference vessel 8 inside the thermostat 6 with the help of pneumatic lines 2, 3 and shutoff valves 4, 5. Differential pressure meter 9 is installed between the vessels. Initial compressed air parameters are fixed in the reference vessel, and current parameters are fixed in the compensating vessel per certain period of time, and thermostat maintains positive temperature balance with the environment.

Below is a sequence of preparatory operations for the leakage testing:

- the device under the test, compensating vessel and reference vessels are filled with compressed air up to the operating pressure;
- operating pressure is aligned throughout the

whole system, and the system is shut off from the compressed air source by the valve 4 (not shown in the Figure 1);

– compressed air temperature in the vessels is stabilized up to specified value, and the reference vessel is shut off from the device under the test; the compensating vessel is still connected to the device, and both vessels are connected to each other through the differential pressure meter.

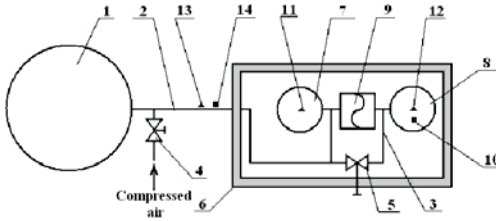


Figure 1. Functional arrangement for testing device for leakage with the help of the fixed-volume method: 1 – device under the test; 2, 3 – pneumatic lines; 4, 5 – shutoff valves; 6 – thermostat; 7, 8 – compensating and reference vessels; 9 – differential pressure meter; 10 – sensor of the gas absolute pressure in the reference vessel; 11, 12, 13 – temperature sensor; 14 – barometric-pressure sensor.

The following measurements are made in real time mode:

- absolute air pressure in the reference vessel – by the sensor 10;
- air temperature in the geometric centers of the reference and compensating vessels – by the sensors 11 and 12;
- environment temperature in the entry to the thermostat – by the sensor 13;
- atmospheric pressure – by the sensor 14 and differential pressure between the compensating and reference vessels – by the sensor 9.

The layout of the reference vessel 8, compensating vessel 7 and differential pressure meter 9 in the thermostat 6 (Figure 1) allows aligning temperature fields in them and removing temperature disturbance received from the device 1. Thank to this, the compensating vessel receives from the device 1 only disturbance caused by differential pressure of compressed air. Changes of the air parameters can be explained by two factors: leakages in the device 1 and changed environment parameters. The changes occur in accordance with the Clapeyron-Mendeleev equation for the gas state and the law of mass and energy conservation.

The mathematic model of testing the devices for leakage by the fixed-volume method is based on the key laws of molecular-kinetic theory of gas (Ginsburg 1966 & Loistyankiy 1973).

Generally, processes occurring in the “device-

compensating vessel” system are described by the following set of equations:

$$\left. \begin{aligned} PV_c &= m_{\kappa,n} RT_{\kappa,c}; \\ PV_t &= m_{u,n} RT_{u,i}; \\ (P + \Delta P_c) V_c &= (m_{\kappa} + \Delta m_{\kappa}) (T_{\kappa,i} + \Delta T_{\kappa,c}) R; \\ (P + \Delta P_c) V_t &= (m_{u,n} + \Delta m_t) (T_{u,i} + \Delta T_{u,c}) R, \end{aligned} \right\} \quad (1)$$

where  $P$  – pressure of compressed air at the beginning of testing (boost pressure);  $V_t$  and  $V_c$  – volumes of the device under the test and compensating vessel;  $m_{\kappa}$  and  $\Delta m_{\kappa}$  – air mass in the compensating vessel at the beginning of testing and its changes in the course of testing;  $T_{\kappa,i}$  and  $\Delta T_{\kappa,c}$  – initial and current temperature in the compensating vessel;  $R$  – universal gas constant;  $m_t$  and  $\Delta m_t$  – air mass in the device at the beginning of testing and its changes in the course of testing;  $T_{u,i}$  and  $\Delta T_{u,c}$  – initial and current temperature in the device;  $\Delta P_c$  – current differential pressure between the compensating and reference vessels measured by differential pressure meter.

This method of leakage test with the help of compensating and reference vessels is based on the assumption that when there is no compressed air leakage from the system mass of the compensating vessel does not change. This conclusion is proved by the equations of the gas state for the compensating vessel at the beginning and at the end of testing when the given gas volume is in the equilibrium state. Equation 1 and 3 of the set (1) shows that:

$$\frac{\Delta m_{\kappa,t}}{m_{\kappa}} \left( 1 + \frac{\Delta T_{\kappa,c}}{T_{\kappa,i}} \right) = \frac{\Delta P_c}{P} - \frac{\Delta T_{\kappa,c}}{T_{\kappa,i}}. \quad (2)$$

From the latter equation, it is obvious that  $\Delta m_{\kappa,t} = 0$ , provided:

$$\frac{\Delta P_c}{P} = \frac{\Delta T_{\kappa,c}}{T_{\kappa,i}} \quad \text{or} \quad \frac{\Delta P_c}{\Delta T_{\kappa,c}} = \frac{\Delta P}{T_{\kappa,i}}.$$

Thus, if there is no leakage in the system ( $\Delta m_{\kappa,t} = 0$ ) though temperature changes due to the heat exchange between the device under the test and environment then the  $\Delta P$  change caused by this temperature factor is linearly connected with the  $\Delta T_{\kappa,c}$  change in the compensating vessel. As pressure in the vessel cannot be less than pressure in the device (it would contradict the Pascal law on the isometry of pressure) the mass can flow only from the compensat-

ing vessel into the device and not vice versa. Therefore, in the equation (2) the  $\Delta m_{\kappa,t}$  is always  $\leq 0$ .

Consequently, as during the time period needed for estimating leakage proofness of the device we have the following correlation:

$$\frac{\Delta P_c}{\Delta T_{\kappa,c}} = \frac{P}{T_{\kappa,i}} = const,$$

then we can say about complete leakage proofness of the device with accuracy commensurable with the measurement inaccuracy.

Distinctive features of this method (they were confirmed by mathematic model during studying physical process of the compressed air leaking from the device under the test) are the following:

1. Re-distribution of the compressed air parameters in the compensating vessel is determined by the adiabat law with adiabat ratio  $k$ , and re-distribution of gas parameters in the device – by polytropy law with polytrophe index  $n$ :

$$\frac{P + \Delta P_c}{P} = \left( \frac{m_{\kappa} + \Delta m_{\kappa,t}}{m_{\kappa}} \right)^k;$$

$$\Delta m_y = \frac{V_t (P + \Delta P_c) \rho_n T_n}{T_{a,i} P_n} \left[ \left( 1 + \frac{T_{t,i} (\Delta P_c - \Delta P_{i,c}) - P (T_{e,t} - T_{t,i})}{P T_{e,t}} \right)^{k/n} - 1 \right] - \frac{T_{t,i} (\Delta P_c - \Delta P_{i,c}) - P (T_{e,t} - T_{t,i})}{T_{t,i} T_{e,t}} \frac{V_e}{R},$$

where  $V_e = V_c$  – volume of the reference vessel;  $\rho_n$ ,  $P_n$ ,  $T_n$  – air density, pressure and temperature at normal conditions which are chosen from the reference data;  $T_{a,i}$  – initial temperature of atmospheric air measured in the entry into the thermostat;  $T_{t,i}$  – initial temperature measured in the compensating vessel;  $\Delta P_{i,c}$  – computed correction for pressure variation under the impact of environment temperature.

Mean value of the current compressed-air temperature in the vessels and correction for pressure variation are calculated by the following formulas:

$$T_{e,t} = T_{\kappa,i} + \Delta T_{\kappa,c} - \Delta T_{e,t};$$

$$\Delta P_{i,c} = P \left( \frac{T_{a,c}}{T_{a,i}} - 1 \right),$$

$$\frac{P + \Delta P_c}{P} = \left( \frac{m_t + \Delta m_{u,i}}{m_t} \right)^n;$$

$$n = \frac{\lg^{P_{a,c}} / (P + \Delta P_c)}{\lg^{P_{a,c}} / (P + \Delta P_c) + \lg^{T_{e,t}} / T_{a,c}},$$

where  $P_{a,c}$  – measured current atmosphere pressure;  $T_{e,t}$  – mean value of the current compressed-air temperature measured in the compensating and reference vessels;  $T_{a,c}$  – current atmosphere pressure measured in the entry into the thermostat.

2. Changed compressed air mass in the device includes air mass flowing out from the device due to the leakage and some quantity of air flowing into the device from the compensating vessel.

3. Mass value  $\Delta m_y$  of factual leakage in the device in the atmospheric condition is determined by the following equation:

where  $\Delta T_{e,t}$  – current change of temperature measured in the reference vessel;  $T_{a,c}$  – current temperature of environment.

In spite of impact of external factors (heat exchange between the device under the test and environment and real variations of pressure) mass value of factual leakage in the device  $\Delta m_y$  depends only on re-distribution of the compressed air mass between the device and compensating vessel. In order to determine  $\Delta m_y$  in the formula (3) impact of changed external factors and steadiness of thermostat operation are taken into account in the polytrophe index  $n$  and values of  $\Delta P_{i,c}$ ,  $T_{t,i}$  and  $T_{e,t}$ .

The mathematic model is based on the following assumptions:

- only quasi-statistic processes are considered;
- relaxation period is essentially less than time periods for which gas-state equations are written;

– time period during which pressure of compressed air in the device changes due to the leakage in the device and heat exchange with the environment is essentially longer than the relaxation period;

– compressed air pressure and its changes are the same in all points of the system according to the Pascal law;

– compressed air temperature and density can differ in different points in the device volume and are inversely dependent on each other;

– compressed air temperature in the pneumatic line in the entry into the thermostat is equal to temperature of environment;

– leakage in the pneumatic line, shutoff valve, compensating and reference vessels and instrumentation equipment is essentially less than measured leakage of compressed air.

Depending on how compressed air mass in the reference vessel has changed factual value of leakage in the device is determined by specially designed fixed-volume method and with taking into account character of changes of environment parameters.

For the purpose of practical testing devices for leakage by the fixed-volume method, the Institute of Geotechnical Mechanics under the National Academy of Science of Ukraine together with the Yuznoye State Design Office named after M.K. Yangel created and tested on the space-rocket hardware a precision Leak Testing Device for Hollow Wares (LTDHW), which consists of the following key structural elements:

– compensating and reference vessels designed as the Dewar spherical container;

– electronic unit for measuring local temperature in gaseous media by quartz frequency thermometers (QFT);

– electronic unit for measuring differential pressure between the vessels which consists of low-limit differential pressure sensor, series LPX/LPM, produced by the “DRUCK Company (UK), and AD converter;

– electronic unit for measuring excess pressure and barometric pressure which consists of two resonance pressure sensors of extra accuracy, RPT series, produced by the “DRUCK Company (UK), and

AD converter. To measure barometric pressure, barometric pressure sensor RPT 410F is used. To measure excess (working) pressure, pressure sensor RPT 200 is used.

The instrumentation equipment has passed incoming metrological inspection and metrological attestation in the National Scientific Center “Metrology Institute”.

At working pressure up to 0.3 MPa (3 kgf / cm<sup>2</sup>), the LTDHW detects factual leakage in the device under the testing with error not more than 20% from the measured values. The low limit of the leakage size measured by the working example of the LTDHW is 10 l micron HG / s. Total time period needed for testing device for leakage is not more than 8 hours.

### 3 CONCLUSIONS

The method to test pneumatic equipment in mines for compressed air leakage with the help of the fixed-volume method is a result of complex theoretical and experimental studies of various methods of detecting micro leakages without using indicating gases and barometric equipment. The fixed-volume method improves accuracy and reliance of detecting compressed-air leakage from the wares of any configuration and helps to determine factual size of total leakage in the devices in real testing conditions. Computerized method of the leakage tests on the basis of the proposed fixed-volume method will provide proper test control, automatic measurement of all parameters, computer processing of measuring results with their conversion to any needed dimensions. The method also makes shorter testing time and improves accuracy and reliance of measurement of factual leakage size in the devices.

### REFERENCES

- Ginsburg, I.P. 1966. *Aerogas dynamics*. Moscow: Vysha shkola.
- Loistyankiy, L.G. 1973. *Fluid and gas mechanics*. Moscow: Nauka.

## Optimal parameters of wall bolts computation in the united bearing system of extraction workings frame-bolt support

V. Bondarenko & I. Kovalevs'ka

National Mining University, Dnipropetrovs'k, Ukraine

R. Svystun

Mokryanskiy quarry, Zaporozhye, Ukraine

Yu. Cherednichenko

"Fuel-energy company of Donetsk" Donets'k, Ukraine

**ABSTRACT:** Engineering approach of required rational parameters of wall bolts installation, which provide optimal load on the frame support all over its contour in view of their mechanical interrelation in the united bearing construction using spatial-flexible units is developed.

Conducted researches of frame-bolt support interaction with rock massif around extraction workings, which are exposed to the intensive impact of stoping, stresses into the support, caused by loads of rock massif computation, obtained solutions numerical analysis allowed to work out engineering approach of flexible frame-bolt support rational parameters. It is based on nomograms range creation, which allows to compute parameters efficiently and accurate enough depending on mining environment and mine engineering conditions of extraction working maintenance. Main design parameters of frame-bolt support include: reactions  $N_j$  of bolts interaction (equal within their bearing ability), coordinates  $\theta_{N_j}$  of bolts installation.

*Computation of impact required reaction on flexible bolts frame props.* Nomogram used to measure required reaction  $N_1$  of bottom bolt, located from the side of the coal seam is shown on Figure 1. Numerical analysis has shown, that required rate of bolts reaction  $N_1$  essentially (more than 10% of  $N_1$  intensity) depends on variables:  $\varphi$ ,  $\varphi_c$ ,  $\frac{k}{q_v}$ ,  $\frac{m}{r}$ ,  $\frac{h}{r}$ . Here,  $\varphi$  and  $\varphi_c$  are the angle of internal friction of rocks and coal, respectively;  $q_v$  and  $k$  – are the vertical load on the frame and the coefficient of its skewness (Bondarenko, Kovalevs'ka & Symanovych 2012), respectively.

Computation of parameter  $\frac{N_1}{q_v r}$  is conducted in terms of quadrants I-V in accordance with wrench move for following basic data:  $\varphi = 30^\circ$ ,  $\varphi_y = 20^\circ$ ,  $\frac{h}{r} = 0.3$  and  $\frac{m}{r} = 0.4$  (which with working arch radius  $r = 2.5$  m corresponds to the height of rock bankette  $h = 0.75$  m and of the seam  $m = 1$  m),  $\frac{k}{q_v} = 0.4$ . From I quadrant's horizontal scale and point  $\varphi = 30^\circ$  we drop a perpendicular to meet with the line  $\frac{h}{r} = 0.3$ , from which we contour in quadrant II up to meet with the line  $\frac{m}{r} = 0.4$ ; from this point we drop a perpendicular to the lower border of the quadrant II, where we receive point  $A$ . From the mark  $\varphi_c = 20^\circ$  on the vertical scale of quadrant IV we contour to the point of meeting with line  $\frac{m}{r} = 0.4$ , from which we erect a perpendicular to the top border of the quadrant IV and receive a point  $B$ . We connect points  $A$  and  $B$  with line we receive intermediate parameter value 0.235 on the summarizing scale of the quadrant 3. We put this value on quadrant's V vertical scale. From this point we contour to the point of meeting with the line



$\frac{k}{q_v} = 0.4$ , from which we erect a perpendicular to the top horizontal scale of quadrant V, where we read the answer  $\frac{N_1}{q_v r} = 0.285$  m. Bottom bolt reaction magnitude  $N_1$  (for example with  $r = 2.5$  m and  $q_v = 165$  kPa) builds up  $N_1 = 0.285 \text{ m} \times 2.5 \text{ m} \times 165 \text{ kPa} = 117 \text{ kN}$  in terms of one frame installation on one long meter of the working. If the number of frames on one long meter equals one, that means  $n = 1$  that the reaction  $N_1$  of the bottom bolts is 117 kN. With other value  $n$  of frames installation on working long meter number reaction  $N'_1$  of the bolt equals

$$N'_1 = \frac{N_1}{n}$$

Nomogram used to measure required reaction  $N_2$  of the top bolt, located from the side of the coal seam is shown on Figure 2. Computation is conducted in accordance with wrench move over the quadrants I-V by analogy with nomogram of reaction  $N_1$  computation. Parameter value  $\frac{N_2}{q_v r}$  for the top bolt (located from the side of the coal seam) builds up 0.20 m. for previously shown basic data, and reaction magnitude  $N_2$  (with  $r = 2.5$  m and  $q_v = 165$  kPa) equals  $N_2 = 0.20 \text{ m} \times 2.5 \text{ m} \times 165 \text{ kPa} = 83 \text{ kN}$  for one long meter of the working.

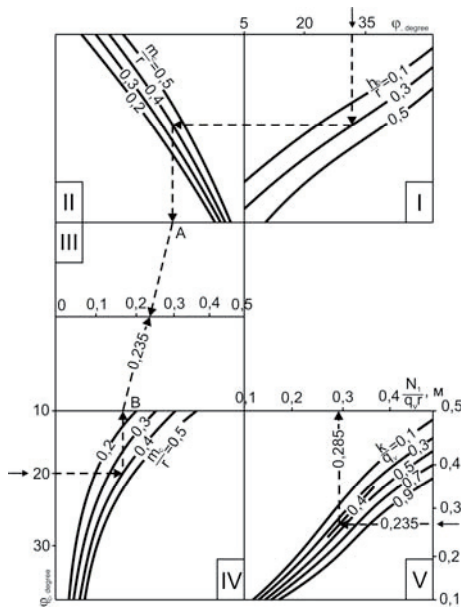


Figure 1. Nomogram used to measure required reaction  $N_1$  of the bottom bolt, located from the side of the coal seam.

Nomogram used to measure required reaction  $N_4$  of the bottom bolt, located from the side of the goaf is shown on Figure 3. Parameter  $\frac{N_4}{q_v r}$  dimensioning is carried out in accordance with wrench move over the quadrants I-V for basic data:  $\varphi = 30^\circ$ ,  $\frac{h}{r} = 0.3$ ,  $\frac{(q_b)_3}{q_v} = 2.0$ ,  $\frac{(q_b)_2}{q_v} = 0.5$ ,  $\frac{m}{r} = 0.4$ ,  $\frac{k}{q_v} = 0.4$  and

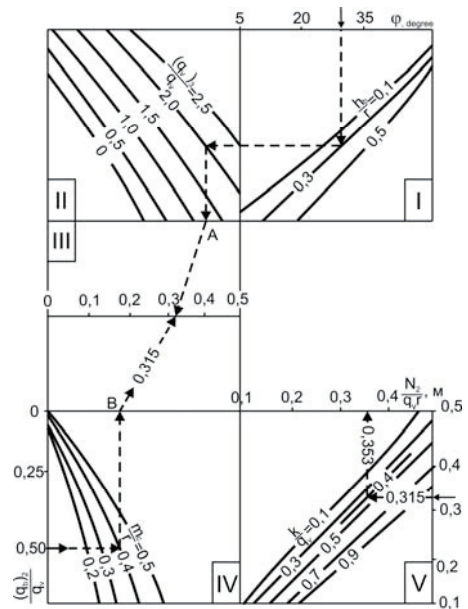


Figure 2. Nomogram used to measure required reaction  $N_2$  of the top bolt, located from the side of the coal seam.

is run in the following order. From the mark  $\varphi = 30^\circ$  on the horizontal scale of quadrant I we drop a perpendicular to meet the line  $\frac{h}{r} = 0.3$ , from which we contour in quadrant II to the line  $\frac{(q_b)_3}{q_v} = 2.0$  and from the point of meeting we drop a perpendicular to the bottom border of the quadrant II, where we re-

ceive point  $A$ . From the value  $\frac{(q_b)_2}{q_v} = 0.5$  on the vertical scale of quadrant IV we contour to the point of meeting with the line  $\frac{m}{r} = 0.4$  and erect a perpendicular to the top border of the quadrant IV, where we receive point  $B$ . Then we connect points  $A$  and  $B$ , and compute value of the intermediate parameter on the horizontal scale of the quadrant III that equals 0.315. We put this value on the vertical scale of quadrant V, and contour to the point of meeting with

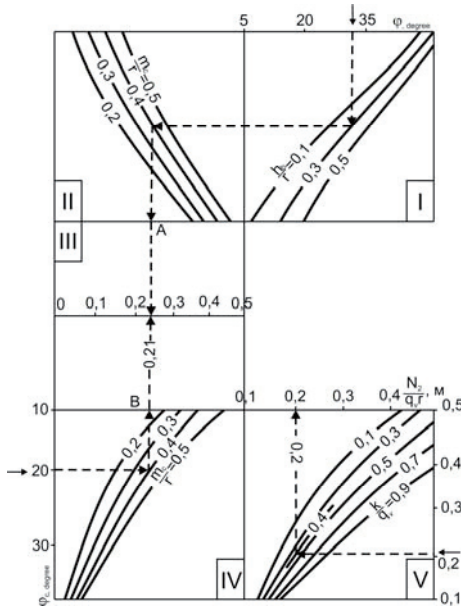


Figure 3. Nomogram used to measure required reaction  $N_4$  of the bottom bolt, located from the side of the goaf.

In order to compute top bolt required reaction  $N_3$ , located from the side of the goaf, nomogram was designed (Figure 4). Usage rules of it are similar to the previous example. A value  $\frac{N_3}{q_v r} = 0.255$  m is received for previously shown basic data, and reaction  $N_3$  magnitude built up  $N_3 = 105$  kN per one long meter of the working.

*Units of flexible bolts connection on frame support props installation place computation.* Except of the required bolts reaction stresses  $N_j$ , rational parameters of their installation also include coordinates of their location over the working contour.

the line  $\frac{k}{q_v} = 0.4$ , from which we erect a perpendicular to the horizontal scale of the quadrant V, where we read the answer  $\frac{N_4}{q_v r} = 0.353$  m. Bottom bolt reaction magnitude  $N_4$  (for example with  $r = 2.5$  m and  $q_v = 165$  kPa) builds up  $N_4 = 0.353$  m  $\times$  2.5 m  $\times$  165 kPa = 145 kN on one long meter of the working.

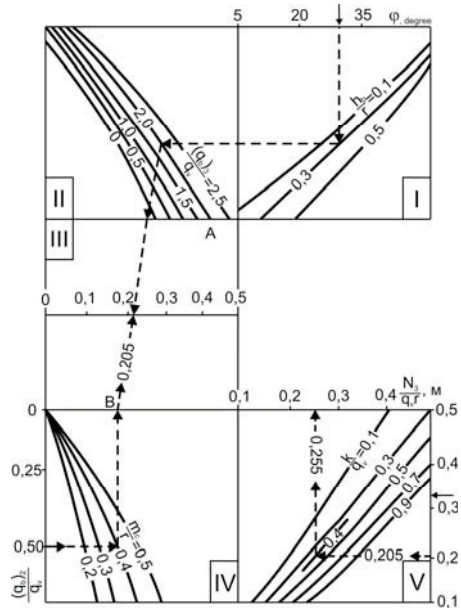


Figure 4. Nomogram used to measure required reaction  $N_3$  of the top bolt, located from the side of the goaf.

Angular coordinate  $\theta_{N_j}$  ( $j=1, \dots, 4$ ) is used as such parameter. According to the analysis, it essentially depends on existing variables: angle of internal friction of rocks  $\varphi$ ; ratio of  $\frac{h}{r}$  natural bankette height to the working arch radius; ration  $\frac{m}{r}$  of seam height to the radius of working arch; angle of internal friction of  $\varphi_c$  coal seam; ratio of  $\frac{k}{q_v}$  load increment  $k$  in zone of stoping influence to the vertical load  $q_v$  on the support out of this zone.

Following variables need to be considered during the computation  $\theta_{N_j}$  for the other pair of bolts ( $j=3,4$ ), that are installed from the side of the goaf: ratio of  $\frac{(q_b)_3}{q_v}$  wall load  $(q_b)_3$  along the length of natural bankette (under security element) to the vertical one  $q_v$ ; ratio  $\frac{(q_b)_2}{q_v}$  of wall load  $(q_b)_2$ , acting along the height of the security element to the vertical one; ratio  $\frac{k}{q_v}$ , angle of internal friction of rock  $\varphi$ ; ratio of  $\frac{h}{r}$  and  $\frac{m}{r}$ .

Nomogram used to compute rational coordinates  $\theta_{N_1}$  of bottom bolt installation over the quadrants I-V is presented on Figure 5 in accordance with wrench move for following basic data:  $\varphi = 30^\circ$ ,  $\varphi_y = 20^\circ$ ,  $\frac{k}{q_v} = 0.4$ ,  $\frac{h}{r} = 0.3$ ,  $\frac{m}{r} = 0.4$ .

From the mark  $\varphi = 30^\circ$  on the vertical scale of quadrant I we contour to the point of meeting with

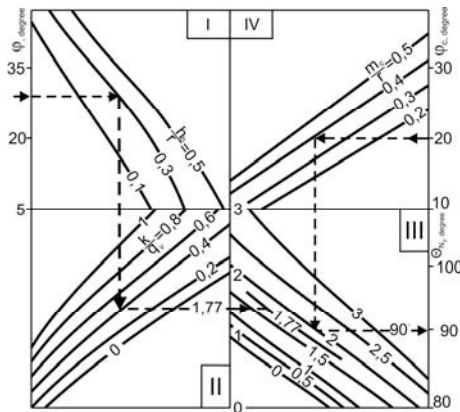


Figure 5. Nomogram used to measure rational coordinate  $\theta_{N_1}$  of the bottom bolt, located from the side of the coal seam.

Nomogram used to Figure rational value  $\theta_{N_3}$  of the top bolt installation, located from the side of the goaf is shown on Figure 7. Computation is conducted in accordance with wrench move for following basic data:  $\frac{(q_b)_3}{q_v} = 0.8$ ,  $\frac{(q_b)_2}{q_v} = 0.4$ ;  $\frac{k}{q_v} = 0.4$ ;  $\varphi = 30^\circ$ ;

the line  $\frac{h}{r} = 0.3$ ; from this point we drop a perpendicular to quadrant II till it meets the line  $\frac{k}{q_v} = 0.4$ , from which we contour to the quadrant II, where we receive value 1.77 of accessory parameter. According to this value we build a curve in quadrant III. From the mark  $\varphi_c = 20^\circ$  in quadrant IV we contour to the line  $\frac{m}{r} = 0.4$ , from which we drop a perpendicular to quadrant III to the built by us line 1.77. From the point of meeting we contour to the right vertical scale of quadrant III, where we read the answer  $\theta_{N_1} = 90^\circ$ . As the result, it is the most rational to install the bottom bolt near the frame bolt arch footing for the given example.

Rational coordinate  $\theta_{N_2}$  of top bolt installation computation from the side of the coal seam is conducted according to the nomogram (Figure 6) similarly to above described example. As a result of computation for the same basic data we discover, that the top bolt must be installed at the angle of  $\theta_{N_2} = 38.6^\circ$  to the working vertical axis.

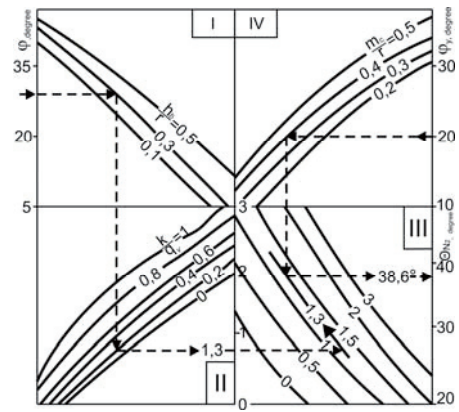


Figure 6. Nomogram used to measure rational coordinate  $\theta_{N_2}$  of the top bolt, located from the side of the coal seam.

$\frac{h}{r} = 0.3$ ;  $\frac{m}{r} = 0.4$ . The other parameters do not have such significant impact on the angular coordinate  $\theta_{N_3}$ . Method of computation is following: from the mark  $\frac{(q_b)_3}{q_v} = 0.8$  of the horizontal scale of quadrant

and we drop a perpendicular to the line  $\frac{h}{r} = 0.3$ ; then we contour in quadrant II to the line  $\frac{(q_b)_2}{q_v} = 0.4$ ; after that we drop a perpendicular to quadrant III to the line  $\frac{m}{r} = 0.4$ ; then we contour from this mark and read on the vertical scale of quadrant III the answer for intermediate parameter. It equals 1.08. After that we contour from the mark  $\varphi = 30^\circ$  on the

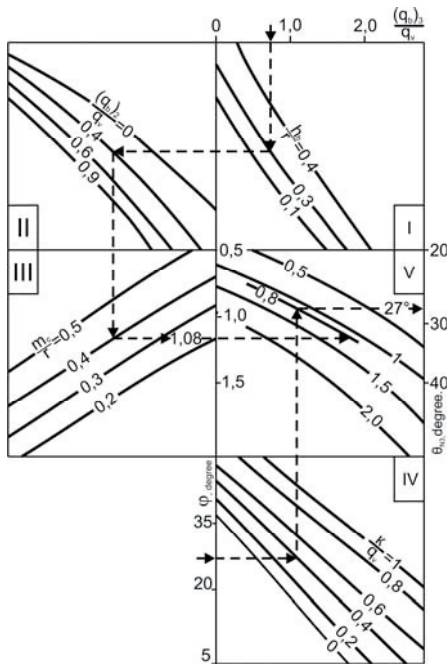


Figure 7. Nomogram used to compute installation coordinate  $\theta_{N_3}$  of the top bolt, located from the side of the goaf.

Thus, as the result of wall bolts and frames unification by means of mechanical bonds into the united bearing system it is possible to create frame-bolt supports in terms of high wall loads. They are notable for reduced material capacity and sufficient bearing ability.

vertical scale of quadrant IV to the line  $\frac{k}{q_v} = 0.4$ , there we erect a perpendicular in quadrant V; we read the answer  $-\theta_{N_3} = 27^\circ$  from the point of meeting of vertical wrench with the line 1.08 in quadrant V on its vertical scale. We compute bottom bolt  $\theta_{N_4} = 95^\circ$  coordinate using nomogram shown on Figure 8 by analogy with the previous one.

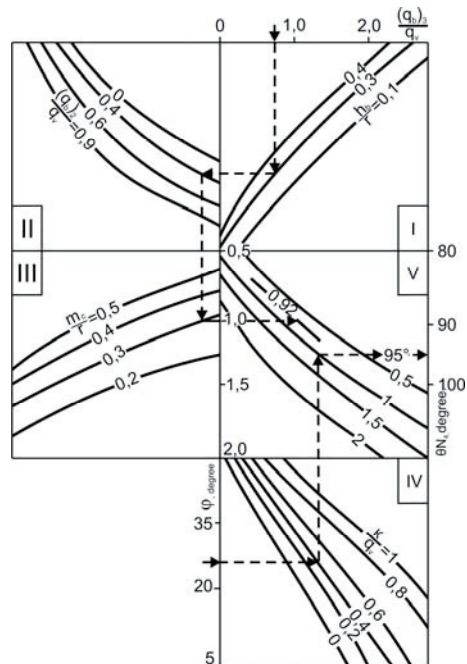


Figure 8. Nomogram used to compute installation coordinate  $\theta_{N_4}$  of the bolt, located from the side of the goaf.

## REFERENCES

- Bondarenko, V., Kovalevs'ka, I., Symanovych, G. and other. 2012. *Process operator guide of extraction working maintenance and security at flat seams*. Research and practice guide. Dnipropetrovs'k: NMU: 98.



# Taylor & Francis

Taylor & Francis Group

<http://taylorandfrancis.com>

## Pillars sizing at magnetite quartzites room-work

M. Stupnik, V. Kalinichenko & S. Pismennyi  
 Kryvyi Rig National University, Kryvyi Rig, Ukraine

**ABSTRACT:** The methods of the inclined pillars parameters calculation at level room-work of thick complex-structural magnetite quartzite deposits in Kryvyi Rig iron ore basin is given.

### 1 SCIENTIFIC AND PRACTICAL TASKS

In Kryvyi Rig iron ore basin rich and poor iron deposits are generally mined by room-work or sublevel caving methods (Table 1).

The main efficiency indices of mining methods are production costs, which is largely determined by the level of ore losses, degree of waste rock dilution and the specific volume of the access workings (Table 2).

Table 1. Mining methods applied in mines.

Enterprise	Mine	Mining depth, m	Mining methods
PJSC “Krivbaszhelezorudkom”	Rodina	1315	sublevel ore caving
	Octyabrskaya	1190	sublevel ore caving; room and pillar caving
	Lenin mine	1275	
	Gvardeiskaya	1270	
PJSC “ArcelorMittal Kryvyi Rig”	#1 Artem mine	1135	sublevel ore caving
PJSC “Evraz Sukha Balka”	Yubileynaya	1260	sublevel ore caving;
	Frunze mine	1135	room and pillar caving

Table 2. Technical and economic indices of mining methods in Kryvyi Rig iron ore basin.

Name	Mining methods		
	Level room-work	Sublevel room-work	Sublevel caving
Specific weight in annual production, %	35.0	20.0	45.0
Specific volume of development and access workings m / th. t	1.9-3.0	2.5-4.5	3.0-5.0
Ore losses, %	5.0-10.0	7.0-12.0	14.7-18.0
	17.4-25.0	16.9-20.0	
Ore dilution, %	4.0-7.0*)	4.0-6.0*)	16.5-18.0
	13.0-16.0*)	11.4-14.0*)	
Iron content reduction in ore output, %	0.5-2.0	0.3-1.5	1.5-3.0

Note: \* – without pillar and ceiling mining.

Table 2 represents that the sublevel caving methods reduce iron ore content in ore output almost by two times in comparison with the room-work (Hivrenko 2001 & Development of technological... 2012). Taking into account that magnetite quartzite deposits are composed of very thick hard rocks technological advancement of their room-and-pillar methods is rather essential.

### 2 PAPER ANALYSIS

Iron ore deposits in Kryvyi Rig basin, reach the

horizontal area of more than 1500 m<sup>2</sup> and strike length of more than 700 m, of ore bodies ranging in size from 50 to 500 m<sup>2</sup> and strike length from 10 to 75 m. The share of large deposits is 80% from the ore area in the basin. Their thickness varies from 20 to 150 m and more. The ore bodies are extended in the north-east direction and lie at angle from 20 to 80 degrees with the grade of ore from 36 to 64%. Physical and mechanical properties of Kryvyi Rig iron ore basin vary widely. Some mine fields have one or two parallel iron deposits containing about 70% of the reserves of the mine field, others have more than 20 separate ore bodies having a strike

length from 150 to 500 m with the grade of ore from 58 to 64% (Development of technological... 2012).

According to the occurrence iron ore deposits are divided into homogeneous and heterogeneous (Development of technological... 2012 & Bizov 2001). There are inclusions of barren area or ores with low grade quality in heterogeneous deposits. The thickness of barren areas varies from 3.2 to 6 m in some areas to 10.6 m. The specific area of barren inclusions within the level (sublevel) is 10...15-18%. The deposits with the presence of barren area, are usually mined by complete mining, see Table 1.

### 3 THE PROBLEM STATEMENT

Application of traditional mining methods with ore complete mining at ore deposits mining, including barren area inevitably leads to a decline of the ore grade quality from 3 to 10%, which significantly af-

fects the sale price of commercial products and increases the cost of extraction, transportation, hoisting of extracted rock mass and its dressing.

Thereby, the development of improved version of mining methods for deposits with barren area inclusions, allowing to increase the quality of mined ore mass, is an important scientific and technical task for mines.

### 4 MATERIAL PRESENTATION AND RESULTS

Ore deposits of Kryvyi Rig iron ore basin according to their structure can be divided into five types: 1 – without barren area inclusions; 2, 3 and 4 – mining ore area has single; double and triple barren area inclusions; 5 – ore area has combined barren area inclusions, Figure 1.

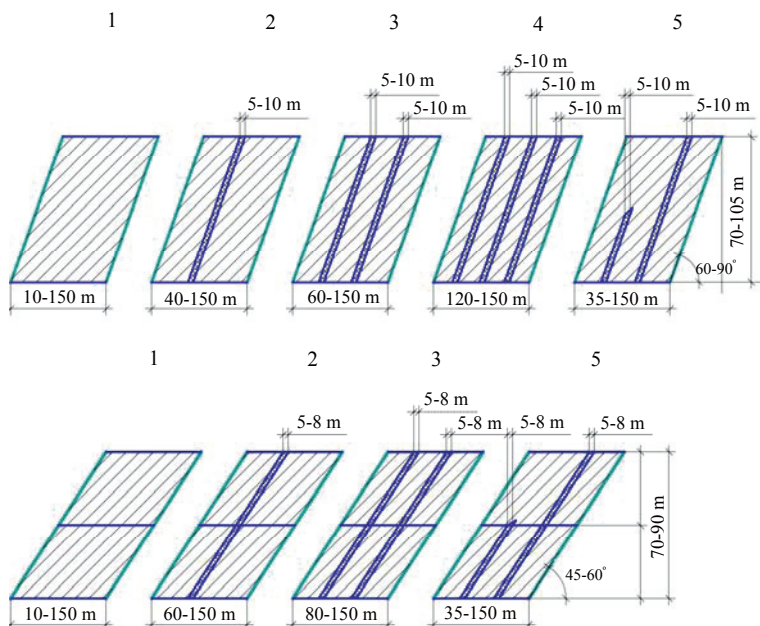


Figure 1. The structure of ore deposits of Kryvyi Rig iron ore basin.

The first type includes all single and parallel and contiguous deposits that don't contain barren area inclusions or the thickness of barren area inclusions between the ore deposits is more than 15 m. In this case, it should be noted that the parallel and contiguous deposits are mined separately. Deposits which have one barren area inclusion with the thickness of not more than 10 m belong to the

second type. The third and the fourth type are ore deposits having two or more barren area inclusions, the distances between barren area inclusions vary from 15 to 35 m and more. The fifth type is ore deposits with barren area inclusions of irregular shape.

Based on researches, the classification of ore deposits of Kryvyi Rig iron ore basin tend to be mined by room and pillar systems is given (Table 3).

Table 3. Morphological classification of ore deposits of Kryvyi Rig iron ore basin.

Name	Without barren area inclusions	Single barren area inclusions		Doubled by barren area inclusion		Tripled by barren area inclusion	Combined barren area inclusions	
	1	2		3		4	5	
Deposit type								
Dip angle of ore deposits, degree	45-90	45-60	60-90	45-60	60-90	60-90	45-60	60-90
Thickness of ore deposits, m	10-150	60-150	40-150	80-150	60-150	120-150	35-150	35-150
Dip angle of barren area inclusions, degree	—	45-90	60-90	45-60	60-90	60-90	45-70	60-90
Thickness of barren area inclusions, m	—	5-8	5-10	5-8	5-10	5-10	5-8	5-10
Rigidity of ore body	+/-	+/-	+/-	+/-	+/-	+/-	+/-	+/-
Rigidity of hanging wall rock	+	+	+/-	+	+	+	+	+/-
Rigidity of bottom wall rock	+	+/-	+	+/-	+	+	+/-	+
Rigidity of rock inclusions	—	+	+/-	+	+	+	+	+/-

Note: + hard ores or rock; – soft ores or rock.

For mining of iron ore deposits with barren area inclusions (type 2-5) it is necessary to use selective mining, leaving barren area inclusions in the waste area (Bizov 2001). This can be achieved by using level (sublevel) room and pillar systems with caving or leaving pillars and crowns between rooms. However, their use has a number of boundary conditions, which include: the minimum allowable thickness of barren area and ore deposit, the amount of mining panels, the thickness of inclined dirt area inclusion (Storchak 2003).

The minimum allowable thickness of barren area inclusion is conditioned by inclined pillar integrity support, normal conditions of ore crashing and determined by

$$m_n \geq 1.5 \cdot W, \quad (1)$$

where  $m_n$  – minimum allowable thickness of barren area inclusion, m;  $W$  – line of least resistance at longhole work, m.

The minimum allowable thickness of ore body limited by the barren area inclusion depends on the underground mining technology, height of level (sublevel) and is determined by

$$m_p \geq (0.1 \dots 0.3) \cdot h \geq m_n, \quad (2)$$

where  $m_p$  – minimum allowable thickness of ore body which is situated near barren area, m,  $h$  – height of level, m.

The amount of mining panels in the stope limited across by barren area inclusions is determined by

$$N = \frac{M}{n} + 1, \quad (3)$$

where  $N$  – amount of mining areas in the stope limited across by barren rock inclusions;  $M$  – horizontal thickness of ore deposit, m,  $n$  – amount of barren area inclusions the thickness of which are ranged from 5 to 8-10m.

The thickness of the inclined barren area inclusion that will ensure its stability for a period of the panel mining is determined by the conditions of the longitudinal compressive forces  $P_l$  in which there is no integrity. Side forces  $P_s$ , are directed towards the previously mined room filled with caved rocks (Storchak 2003). The design formula for determining the width of the inclined interstall pillar is

$$b = \frac{P_l \cdot K_d \cdot \xi \cdot \sqrt{\sigma_t \cdot h}}{n_c \cdot \sigma_{com} \cdot \sqrt{K_f \cdot \gamma}} \geq m_s, \quad (4)$$

where  $P_l$  – longitudinal compressive forces work along the inclined pillar;  $K_d$  – ratio depending on the tensile stress and rock deformation;  $\xi$  – ratio of rock creeping;  $\sigma_t$  – rock tensile strength, kPa;  $n_c$  – amount of longitudinal pillars per one room;  $\sigma_{com}$  – rock compressive strength;  $K_f$  – inclined pillar stability factor;  $\gamma$  – specific weight of rock, forming the inclined pillar, kg / m<sup>3</sup>.

In the case when there is no tensile stress and de-



formation in the pillar  $K_d$  is 1.15-1.41, when inclined pillar subjected to maximum deformation without affecting its integrity  $K_d$  is 1.41-1.73, in the laminated fractured ground with possible or partial pillar caving  $K_d$  is 1.63-2.0, and at crack initiation with the following caving  $K_d$  is 2.0-2.44 (Slesarev 1948).

So, the width of the inclined barren pillar defined

by the expression (4) should be 1.5 times greater than the thickness power of barren area inclusion. As a result of researches an improved version of the level room mining methods with pillars and crown caving is developed.

A distinctive feature of the proposed version of the room mining method shown in Figure 2, from the traditional is the following. Mining section is divided into mining panels according to the thickness.

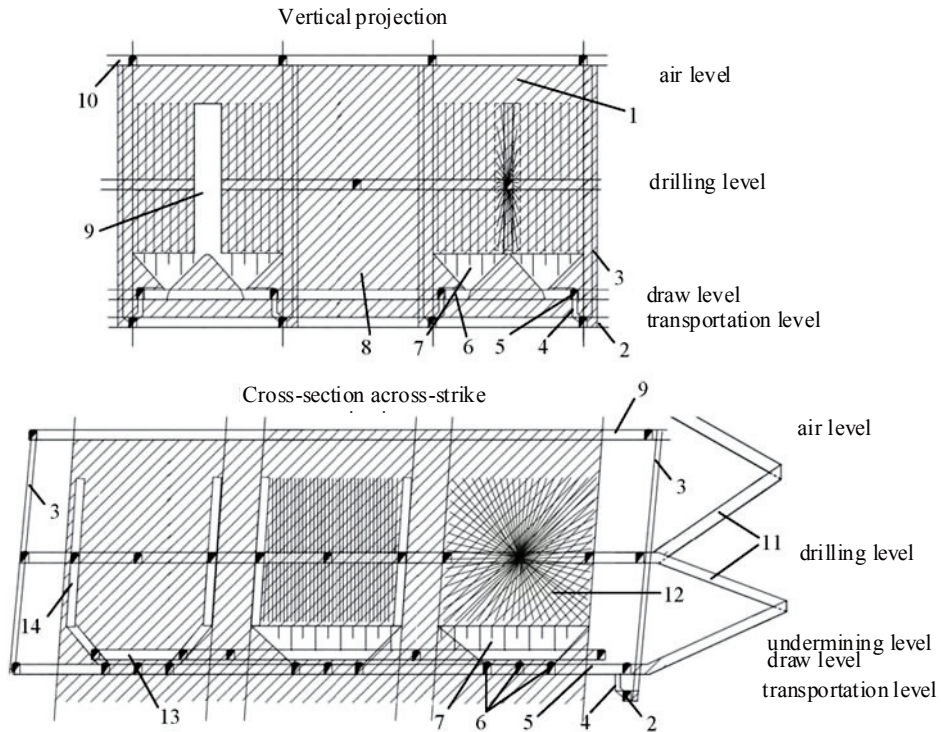


Figure 2. Level room development with dirt inclusions leaving in the section: 1 – primary stope (room); 2 – hauling roadway; 3, 4 – raise, air and passageway, ore-pass; 5, 10 – draw entry; 6 – loading rooms; 7 – ditch undercutting; 8 – stope of the second turn (room fender); 9 – vertical compensation room; 11 – spiral ramp; 12 – rings of block caving deep holes; 13 – cutoff ditch ort; 14 – cut raise.

The first section is limited by hanging wall rock and hanging wall of barren area inclusion, the last one is limited by hanging wall of barren area inclusion and bottom wall. Section mining is carried out by mining panels from hanging to bottom wall.

The panels are mined separately by level, (sub-level-) room and pillar system with the formation of a separate compensation space, drilling and recei-

ving levels. Between the mining panels the inclined pillar consisting of barren inclusion is left. Interstall inclined pillars (barren inclusions) are not mined but remain unaffected between panels. Ore pillars and crowns mining are carried out according to the traditional technology. The results of calculation of improved mining method application compared with traditional technologies are shown in Table 4.

Table 4. Technical and economic indices of mining methods in deposits with barren area inclusions.

Name	Room and pillar mining without pillar caving	Ore and cover caving methods	Proposal room and pillar mining method
Block (panel) parameters			
Block strike length, m	50	50	50
Mining thickness, m	100	100	80
Level height, m	90	90	90
Barren inclusion thickness, m	10	10	-
Dip angle of ore deposits, degree	80	80	80
Barren inclusions amount, pieces	2	2	-
Mined blocks (panels) amount, pieces	1	1	3
Ore volume weight, t / m <sup>3</sup>	2.8	2.8	2.8
Barren inclusions volume weight, t / m <sup>3</sup>	2.2	2.2	-
Ore mass reserve in the block, th. t	1206	1206	1008
– ore reserve in the block, th. t	1008	1008	1008
– barren inclusion reserve in the block, th. t	198	198	-
Grade, %:			
– in ore	46.0	46.0	46.0
– in rock	24.0	24.0	24.0
– in dirt inclusions	16.0	16.0	-
Specific rate of preliminary development and access working, m / th.	2.8	3.6	3.8
Ore output per hole meter run, ton / m	21	20	25
Output per man-shift, t / per shift	136.2	154.8	155.72
Grade of mining block (panel), %	40.0	40.0	46.0
Ore loss, %	10.0	16.0	10.0
Ore dilution, %	7.0	15.0	7.0
Ore mass amount, th. t	1084.5	1191.8	975.5
Grade of mined ore, %	38.9	37.6	44.5

## 5 CONCLUSIONS

It is determined that the use of inclined pillars consisting of barren area inclusions allows to increase the iron content in the mined ore from 37.6-38.9% to 44.5%, and to reduce drilling, output and minerals processing costs. Thus, the ore output is reduced by 10-18%, which significantly reduces the rock processing and haulage costs.

The given method of pillars determination is applicable when the calculated width of inclined pillars is equal to or less than the barren inclusion thickness. In the case when the calculated width of the inclined pillar is more than the barren inclusion thickness, the traditional ore and cover caving method is applied.

## REFERENCES

- Hivrenko, V. 2001. *Technological classification of complicated structural deposits*. Ore deposits development. Kryvyi Rig: KTU, #76: 26-29.
- Development of technological opening schemes, preparation and longwall mining for complicated structural deposits at further development on big depth*: Report from research work. 2012. #GR 0109U002336. Kryvorizhs'kyi national university, #30-84-11: 306.
- Bizov, V., Storchak, S., Sirichko, V., Cherednichenko, O., Garkusha, A., Vitryak, V., Plothikov, V., Repin, O., Hivrenko, O., Schelkanov, V. & Andreev, B. 2001. *Patent № 37982A E 21 C41/16 UA. Method of steep ore bodies development that consist waste rock insertion*". Publish 15.05.2001. Bulletin #4.
- Storchak, S., Chelkanov, V., Karamanic, F., Andreev, B., Korzh, V. & Pismennyi, S. 2003. *Patent. 62168 UA, MKI E21C41/06. Method of steep deposit development of mineral resources*. Publisher 02.01.2003; Publish 15.12.2003; Bulletin #12.
- Slesarev, V. 1948. *Rock mechanics and mine support*. Moscow: Coal Publisher: 45.



Taylor & Francis

Taylor & Francis Group

<http://taylorandfrancis.com>

## The calculation scheme of mathematical modeling of displacement process of a terrestrial surface by working out of coal layers

M. Antoshchenko, L. Chepurnaya & M. Filatyev  
*Donbass State Technical University, Alchevs'k, Ukraine*

**ABSTRACT:** On the basis of the carried-out theoretical research and analysis of experimental data it's been developed method of forecasting final subsidence of terrestrial surface which uses trajectory displacement of points on the earth surface and which takes into account the mechanical properties of rocks, mining depth and geometry sizes of extraction sites.

Determination of regularities of process of displacement of a terrestrial surface at a side job its clearing developments is one of the main objectives while working off of coal layers. The authentic forecast of parameters of displacement of a terrestrial surface promotes the successful decision of others, not less important, mining tasks. To them, except protection of objects on a terrestrial surface, the choice of the location of excavations and rational ways of their protection from influence of mountain pressure, the gas emission forecast from undermining sources, justification of rational schemes of airing of extraction sites, calculation of bearing ability support also many other things belong. By the solution of the specified tasks essential value has establishment of dynamics of displacement process and allocation of its characteristic stages.

Duration of process is considered the period of time during which the terrestrial surface is in a condition of displacement owing to influence of clearing works. The general duration divides into three stages: initial, active and subsidence stage. Establishment of the specified stages according to the normative document (The rule of undermining of buildings, 2004) is made rather conditionally and in modern conditions of big depths of development to their definition it is impossible to declare existing approach completely correct (Kulibaba 2010). Its main shortcoming is lack of accurate and unambiguous methods of definition of a temporary framework of course, both all process of displacement of a terrestrial surface, and its separate stages. The most perspective direction in the solution of a considered problem it's offered the approach represented by Professor Gavrilenko Yu.N. (Gavrilenko 2007).

Division of displacement process of a terrestrial surface on separate stages is offered to be made by

means of characteristic points of the mathematical function describing development of subsidence of a terrestrial surface in time. By way of such points it is offered to use extremes of the first three derivatives on time from the main equation describing the change of subsidence of a point of a terrestrial surface in the process of displacement (2-4).

By the mathematical models (2-4) it's supposed the formation of a flat bottom displacement trough on a terrestrial surface ( $\eta_0$ ) by carrying out clearing works within one extraction site. It is recommended (Gavrilenko 2011) to take a time point as the end of the process when the current subsidence ( $\eta_0$ ) reaches 0.97-0.99 its final value. At such approach it is possible to consider that depth of a flat bottom displacement trough ( $\eta_0$ ) is equal to final displacement of a terrestrial surface ( $\eta_K$ ), taken for one of main parameters of mathematical models (2-4).

The analysis of known experimental data (Borznych, 1999) showed that there are mining-and-geological conditions in which the flat bottom displacement trough on a terrestrial surface isn't formed even by working out of several extraction sites. It testifies that mathematical models (2-4) adequately describe processes of displacement of a terrestrial surface only for the greatest possible extent of development of clearing works after formation of a flat bottom displacement trough. By their use for forecasting of course of process it's still unknown the value of final subsidence of a terrestrial surface ( $\eta_K$ ). The offer (Gavrilenko 2011) to define ( $\eta_K$ ) according to (The rule of undermining of buildings... 2004) is insufficiently reasonable for the reasons given earlier in work (Kulibaba 2010). Besides this it has been established (Filatyev 2011) that cri-

teria of formation of a flat bottom displacement trough by working out of anthracitic layers significantly differ from recommended (The rule of undermining of buildings... 2004). For the specified reasons in this work the purpose to develop the scheme of subsidence of a terrestrial surface before achievement of its full side job during removal of a clearing face from the cutting furnace is set. Such approach will allow to open more fully features of course of process of displacement of a terrestrial surface and to predict value at any extent of development of clearing works with removal of a clearing face from the cutting furnace on distance of  $L$ .

Processes of displacement of a terrestrial surface are considered by mathematical model (Gavrilenko 2011) in time for approximately identical speed of a moving of a clearing face. Such condition of application of model is noted in work (Kulibaba 2010). The author of the model (Gavrilenko 2011) offers also for the description of development of process of displacement instead of time on abscissa axis to use distance concerning a projection of the line of a clearing face to a terrestrial surface to a supervision point. Use of geometrical parameters, in our opinion, is more expedient as they allow coordinating the extent of development of clearing works, the change of corners of full displacements in the undermining rocks and the maximum subsidence of a terrestrial surface. Confirmation of validity of such approach are also almost functional dependences of the maximum subsidence of a terrestrial surface ( $\eta_m$ ) in specific mining-and-geological conditions by changing of one of the geometrical amount of clearing development (Filatyev 2011) that is explained by constancy of thickness of developed layer ( $m$ ), depth of carrying out works ( $H$ ) and strength properties of undermining rocks. In the conditions of one mining layers, owing to the specified reasons, it is possible to apply mathematical dependences, both with absolute parameters, and with relative ones (Filatyev 2011). Relative parameters ( $\eta_m/m$ ,  $L/H$ ) it is expedient to use for generalization of the results received in different mining-and-geological conditions (Filatyev 2011).

By developing the scheme of formation of trough parameters of displacement of a terrestrial surface (fig. 1) it has been used modern ideas of the geomechanical processes happening in undermining rocks by development of clearing works. They consist of the following:

- the beginning of displacement of a terrestrial surface occurs in a point A during removal of a clearing face from the cutting furnace on some distance  $L_H$ , which is defined by strength properties of

rocks ( $f$ ) and depth of carrying out works ( $H$ ). The scheme of change of a ratio between boundary corners and corners of full displacement in process of development of clearing works is given in the reference (Filatyev 2010);

- the maximum subsidence of a terrestrial surface ( $\eta_m^1, \eta_m^2, \eta_m^3 \dots \eta_m^i$ ) to its full undermining by layers of a flat bedding take place approximately over the middle of the developed space. Dependence  $\eta_m = \varphi_1(L)$  is described by curve 4 (Figure 1). Final subsidence ( $\eta_k^i$ ) for the concrete position of a clearing face (the amount of clearing development) is characterized by the maximum subsidence  $\eta_k^i \approx \eta_m^i$ ;

- the full undermining of a terrestrial surface is observed during removal of a clearing face from the cutting furnace on distance more  $L_K$ . In this case the final, most possible value of subsidence of a terrestrial surface ( $\eta_k$ ) is approximately equal to depth of a flat bottom trough ( $\eta_0$ );

- after formation of a flat bottom trough displacement of any point on a terrestrial surface doesn't depend any more on distance of its projection to the cutting furnace, and is connected only with a further moving of a clearing face. The description of process of displacement of a terrestrial surface during this period of development of clearing works completely corresponds to mathematical models (2-4).

The developed scheme of trough formation of displacement of a terrestrial surface during removal of a clearing face from the cutting furnace is confirmed both direct measurement of some parameters, and their calculation with use of experimental data about the processes which are caused by displacement of undermined rocks and indirectly characterizing their condition.

For example, fixing distances between a clearing face and the cutting furnace and observing dynamics of methane emission in vent wells (excavations), it is possible to calculate the change of corners of unloading (full displacement). In specific conditions the sizes of these corners changed in process of development of clearing works from 35 to 65° (Antoshchenko 2013) that practically corresponds to their final values (The rule of undermining of buildings... 2004).

One of important points is definition of withdrawal of a clearing face from the cutting furnace ( $L_H$ ), by which displacement of a terrestrial surface begins. For specific mining-and-geological conditions it can be defined, having statistically processed experimental data of directly proportional depend-

ences  $\eta_m = \varphi_1(L)$  or  $\eta_m/m = \varphi_2(L/H)$ . Such type of dependences is caused by an active stage of course of process of displacement of rocks during this period of time of clearing works. The point of intersection of these dependences with abscissa axis (A) defines required value  $L_H$ . The example of such definition is given in the work (Antoshchenko 2012) when at  $H = 97 \div 114$  m value  $L_H$  made 21 m.

The key moment for the adequate description of processes by means of mathematical models is establishment of a trajectory of movement of points with the maximum value of subsidence  $\eta_m$  towards a moving of a clearing face. In the scheme offered by us the trajectory of movement of these points corresponds to a curve of 4 (Figure 1). In the

scheme (Antipenko 2001) dependence  $\eta_m = \varphi_1(L)$  is accepted rectilinear. For specification of a type of this dependence by a method of the smallest squares made statistical processing of the experimental data known from references obtained for the last fifty years. The empirical dependences characterizing change of relative maximum subsidence of a terrestrial surface ( $\eta_m/m$ ), are received for different mining-and-geological and mining conditions. Initial grouping of basic experimental data were made on strength properties of containing rocks. The rocks containing anthracitic layers are referred to the strongest. The intermediate group on durability is represented by layers with coals of average degree of a metamorphism. Less strong are rocks of the Western Donbass.

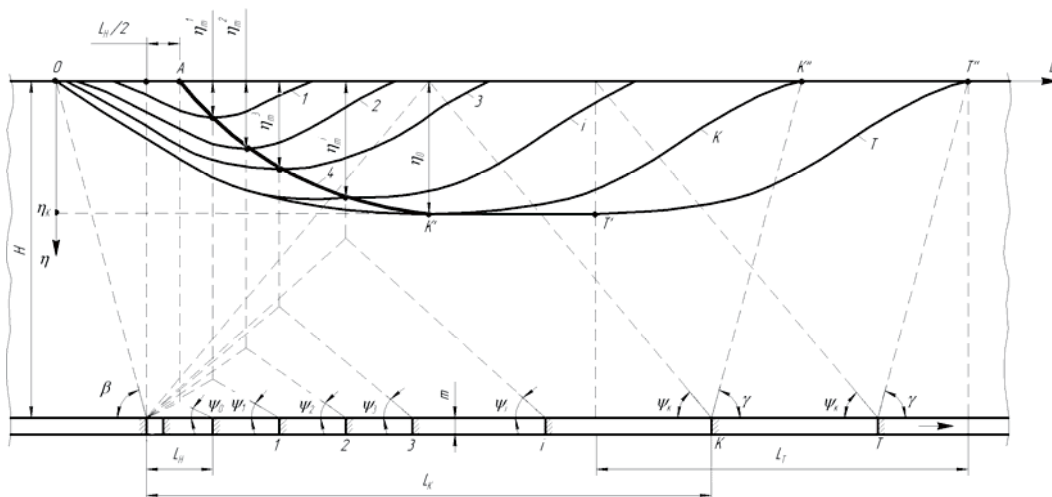


Figure 1. Scheme of formation of trough parameters of displacement of a terrestrial surface during removal of a clearing face from the cutting furnace:  $H$  – depth of carrying out clearing works;  $m$  – thickness of developed layer; 1, 2, 3, ...  $i$ , ...  $\kappa$ , ...  $T$  – the position of a clearing face at its withdrawal from the cutting furnace and trough of subsidence of a terrestrial surface corresponding to them;  $\beta, \gamma$  – boundary corners;  $\psi_0$  – the corner of full displacement corresponding to the beginning of subsidence of a terrestrial surface,  $\psi_1, \psi_2, \psi_3, \dots, \psi_i$  – the corners of full displacement corresponding to 1, 2, 3, ...  $i$  – positions of a clearing face;  $\psi_\kappa$  – final value of a corner of full displacement,  $\eta_m^1, \eta_m^2, \eta_m^3, \dots, \eta_m^i$  – maximum subsidence of the terrestrial surface, corresponding to 1, 2, 3, ...  $i$  – positions of a clearing face; 4 – trajectory of movement of points with the maximum value of subsidence  $\eta_m$  towards a moving of a clearing face;  $\eta_\kappa$  – final subsidence of a terrestrial surface approximately equal to depth of a flat bottom trough of displacement  $\eta_0$ ;  $L_H$  – distance from a clearing face to the cutting furnace at which displacement of a terrestrial surface begins;  $L_\kappa$  – distance from a clearing face to the cutting furnace at which there is a full undermining of a terrestrial surface;  $\rightarrow$  – direction of a moving of a clearing face.

Except strength properties of containing rocks during processing experimental data the depth of carrying out works ( $H$ ) and the amount of clearing developments were considered ( $L_1, L_2$ ). In the

course of experiments one of the geometrical sizes changed, and the second remained constant. If the single lava of variable length  $L_1$  was object of su-

pervision, the change  $\eta_m$  during removal of a clearing face from the cutting furnace on a distance  $L_2$  was considered. By working out of several extraction sites when the full side job of a terrestrial surface wasn't reached, length of an extraction column was invariable. In this case value  $\eta_m$  was defined after discrete increase of the second size of the developed space at the size of length of the next fulfilled lava.

Such approach allowed receiving the empirical equations (1-3) considering two sizes of clearing development:

– for conditions of working out of anthracitic layers

$$\eta_m / m = \frac{0.67}{1 + 9.83 \cdot \exp\left(-2.16 \frac{L_1}{H} \cdot \frac{L_2}{H}\right)}; \quad (1)$$

– by extraction of layers with coals of average degree of a metamorphism

$$\eta_m / m = \frac{0.78}{1 + 11.31 \cdot \exp\left(-3.14 \frac{L_1}{H} \cdot \frac{L_2}{H}\right)}; \quad (2)$$

– for the Western Donbass

$$\eta_m / m = \frac{0.92}{1 + 23.97 \cdot \exp\left(-4.79 \frac{L_1}{H} \cdot \frac{L_2}{H}\right)}. \quad (3)$$

The logistic equations of type (1-3) are usually used for modeling of processes of transition from one stable condition in another. In relation to the description of subsidence of a terrestrial surface the numerator characterizes the greatest possible value  $\eta_m / m$ . In the case under consideration it corresponds to depth of a flat bottom trough of displacement of a terrestrial surface at a stage of carrying out clearing works. Empirical coefficients of a denominator define the position of a curve concerning abscissa axis and width of an average site (an active stage). Dependences (1-3) almost functionally describe processes of displacement of a terrestrial surface and correspond to their physical sense at values  $\frac{L_1}{H} \cdot \frac{L_2}{H} \geq 0.3 \div 0.5$ . Smaller values of argument  $\left(\frac{L_1}{H} \cdot \frac{L_2}{H}\right)$  characterize processes of the beginning of displacement of a terrestrial surface and demand the separate studying.

After removal of a clearing face from the cutting furnace on distance  $L_\kappa$ , a site  $(K' - T')$  of curve

dependence  $\eta_m = \varphi(L)$  becomes almost parallel to abscissa axis (Figure 1) that testifies to formation of a flat bottom displacement trough. Subsidence of a terrestrial surface on a site between points  $T'$  and  $T''$  also is defined by only the current position ( $T$ ) of a clearing face. The distance from a projection of points of a terrestrial surface to the cutting furnace in this case has no any more practical impact on processes of displacement and consolidation of the undermined rocks.

The developed scheme, coordinating development of clearing works and processes of displacement of a terrestrial surface, allows expanding a scope of mathematical modeling by means of characteristic points. On the basis of the carrying out researches the important practical conclusions have been don for mining science:

– in mathematical models instead of temporary parameter more expedient is to use the geometrical sizes of clearing development (the developed space). It will allow developing the general mathematical models for the description of processes of displacement by removing of a certain group of coal layers. In this case it is possible to go to time factor, setting values of speed of a moving of a clearing face;

– three stages of processes of displacement of a terrestrial surface (initial, active and attenuations) have the features connected with development of clearing works. By an incomplete side job of a terrestrial surface it is necessary to consider mathematical models with use of the parameters characterizing the geometrical sizes of clearing developments (the developed spaces). After achievement of a full side job processes of displacement of points of a terrestrial surface depend only on their position in relation to a clearing face;

– for mathematical modeling it is conditionally possible to consider that formation of a flat bottom trough of displacement of a terrestrial surface is one of criteria of the end of processes at a stage of carrying out clearing works;

– final displacement of a terrestrial surface needs to be defined taking into account the sizes of earlier fulfilled extraction sites;

– in the conditions of one mining layer at approximately constant values of depth of carrying out works, the thickness of developed layer and strength properties of containing rocks can be used mathematical dependences both with absolute parameters, and with the relative ones. Relative parameters are recommended to be applied to generalization of the experimental data obtained in different mining-and-geological conditions;

– movement of a trajectory of points towards a moving of a clearing face during its removal from

the cutting furnace happens to the maximum value of subsidence of a terrestrial surface generally on curvilinear dependence that is confirmed by statistical processing of experimental data. The beginning of displacement in this case is determined by a point of intersection of the specified dependences on abscissa axis;

– some parameters of displacement of rocks and a terrestrial surface can be determined on the experimental curve characterizing dynamics of gas emission from underlined sources;

– the choice of mathematical functions for the adequate description of process of subsidence of a terrestrial surface at all stages of development of clearing works by means of characteristic points demands the further analysis and development of recommendations about their application in specific mining-and-geological conditions.

## REFERENCES

- The rule of undermining of buildings, constructions and natural objects at coal mining by underground way. Publishing house is official.* 2004. GSTU 101.00159226.001-2003. Sectoral standard of Ukraine. Kyiv: Ministry of Energy of Ukraine: 128.
- Kulibaba, S.B., Rozhko, M.D. & Hokhlov's, B.V. 2010. *Nature of development of process of displacement of a terrestrial surface in time over moving clearing face.* Science works UKRNDM NAN of Ukraine, 7: 40-54.
- Gavrilenko, Yu.N. 2007. *The mathematical description of dynamics of process of displacement on coal mines of Donbass.* International Society for Mine Surveying, XIII International Congress. Budapest, Hungary. Report 032: 6.
- Gavrilenko, Yu.N. 2011. *Forecasting of displacement of a terrestrial surface in time.* Coal of Ukraine, 6: 45-49.
- Borzych, A.F. & Gorovoi, E.P. 1999. *Influence of width of the developed space on activation of displacement of carboniferous massif.* Coal of Ukraine, 9: 26-30.
- Filatyevev, M.V., Antoshchenko, N.I. & Syatkovsky, S.L. 2011. *About the maximum displacement of a terrestrial surface by working out of coal layers.* Coal of Ukraine, 2: 37-40.
- Filatyevev, M.V. 2011. *Influence of extent of development of clearing works on the maximum subsidence of a terrestrial surface.* Coal of Ukraine, 4: 12-16.
- Filatyevev M.V., Antoshchenko, N.I. & Syatkovsky, S.L. 2010. *Necessary conditions of formation of a flat bottom trough of displacement of a terrestrial surface after removing of coal layers.* Sb. scientific works of DonSTU. Vyp. 31. Alchevs'k: 41-49.
- Antoshchenko, N.I., Kulakova, S.I. & Filatyev, M.V. 2013. *The gas emission forecast from the underlined coal layers.* Coal of Ukraine, 1: 44-49.
- Antoshchenko, N.I., Chepurnaya, L.A. & Filatyev, M.V. 2012. *Quantitative assessment of parameters of displacement of the underlined rocks and a terrestrial surface by removing coal layers.* Sb. scientific works of DonSTU. Vyp. 38. Alchevs'k: 17-24.
- Antipenko, G.A. & Nazarenko, V.A. 2001. *About some terms and definitions of process of displacement of a terrestrial surface.* Coal of Ukraine, 9: 44-45.





# Taylor & Francis

Taylor & Francis Group

<http://taylorandfrancis.com>

## Changes of overburden stresses in time and their manifestations in seismic wave indices

A. Antsyferov, A. Trifonov, V. Tumanov & L. Ivanov  
*UkrSRMI of the NAS of Ukraine, Donets'k, Ukraine*

**ABSTRACT:** During one and a half – two months, due to the redistribution of the stress state, the energy indicator of low-velocity low-frequency waves of channel nature can increase and decrease two-threefold and the energy indicator of high-frequency component of the refracted waves can change by a factor of four.

Coal-producing areas are characterized by manifestations of widespread geodynamic phenomena. Among these are rock bursts, induced earthquakes, ground surface subsidence and caving and others. Unpredictability or poor predictability leads to emergency and catastrophic situations. Occurrence of these phenomena is closely connected with the changes in the stress state of rocks in time. For that reason research into the changes in time of the stress state conducted in coal-producing areas is of immediate interest.

Changes in the stress state are caused by two main groups of factors: natural and human-induced. The main natural factors are recent tectonic fault movements, and undermining of rock mass is human-induced factor.

Estimation of the stress-deformation state of rock mass based on the data of ground surface movement is traditionally used for long-lasting processes. Monitoring of geophysical fields provides information on the changes in the stress state during comparatively short time determined by months, days and hours. In recent times estimation of rock stresses employing seismic sounding techniques grows rapidly (Antsyferov, Tirkel and other 2009; Trifonov, Kiselev and other 2012; Trifonov, Arkhipenko and other 2010; Antsyferov, Trifonov and other 2009; Trifonov, Tirkel and other 2009; & Antsyferov, Tirkel and other 2008 & Antsyferov, Tirkel and other 2007). Prospects of these techniques are specified by parametric abundance of seismic waves and capability of simultaneous use of several types of waves with physically different principles of generation and propagation.

Changes in seismic wave dynamic indices due to a joint impact of fault and rock mass undermining have been detected at the mine field of the Pokrovskoe Mining Unit in the Krasnoarmeisk coal province of the Donets Coal Basin. Surveys were conducted at two areas (area #1 and area #2 located

within the overburden exposure of fault zone of the Kotlinsky overlap fault. The bottom of the overburden lies at the depth of about 40 m. Overlap fault throws in the range of the first tens to the first hundreds meters. Its recent activity is confirmed by geophysical observations conducted in combination with geophysical survey. Both areas are located within subsidence profile, closer to its axial line. Rock mass have been undermined down to the depth of 750 m for one and a half year before surveying began. Taking into account that rock movement has been occurring for several years, the rock mass under consideration is in conditions of the changes in the stress-deformation state.

Sounding was conducted down to the depth of the overburden with the offset recording range of 60 m. Seismic signal generation and recording were carried out in shallow (about 1.0 m) wells with multiple (up to 100 times) stacking based on seismic energy excitation. Three cycles of observations were conducted at two mine field areas repeated in 1.5-2 months (07.08.12; 26.09.12; 20.11.12).

Spectra of the recorded seismic signals are shown in Figure 1. These spectra reflect several types of waves: high-intensity surface waves, refracted and low-velocity low-frequency waves. It is determined that during three cycles of observations changes in the spectrum of seismic signals take place. Sufficiently expressed differences are typical for its high-frequency region. At the area #1 they are confined to the frequency range of 50-70 Hz, and at the area #2 to 45-60 Hz (Figure 2).

With regard to the sounding conditions under examination the described changes in the spectrum is the manifestation of high-frequency components of refracted waves propagating in the deep dense part of the overburden. It is determined that energy index of the spectrum high-frequency components (as the sum of the amplitudes of frequency components of

spectrum ranges) changes considerably during monitoring. At first (cycles 1-2) this index decreases, and then (cycles 1-2) increases. Its change takes place concurrently at two areas and achieves four-fold value (see Figure 2).

Seismic signals as absolute values of the amplitudes reduced by energy index of the first signal phase with averaging the energy index by sliding window method (width = 50 ms, interval = 25 ms) are shown in Figure 3.

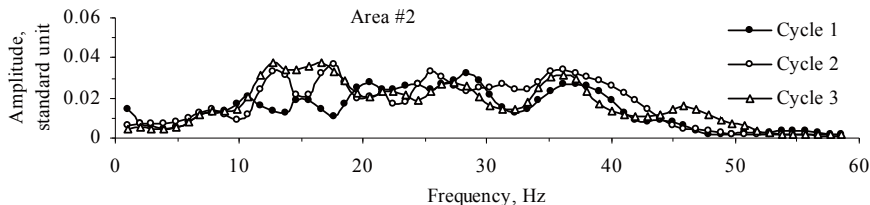


Figure 1. Seismic signal spectra based on three cycles of observations.

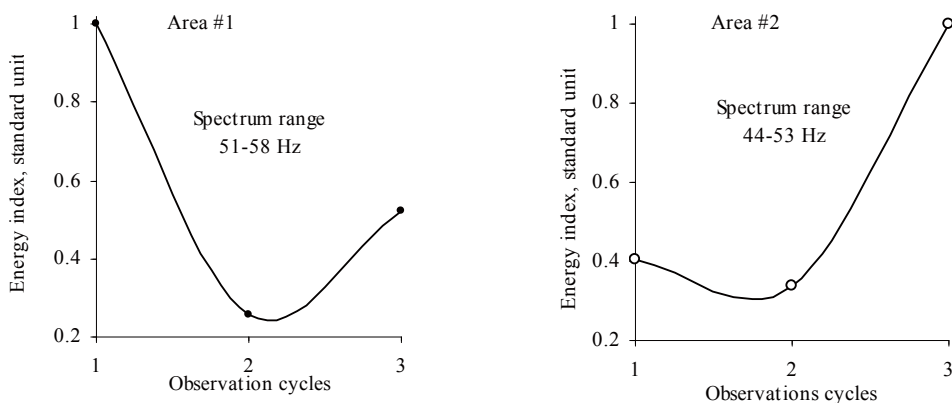


Figure 2. High-frequency part of seismic signal spectra and energy indices based on three cycles of observations.

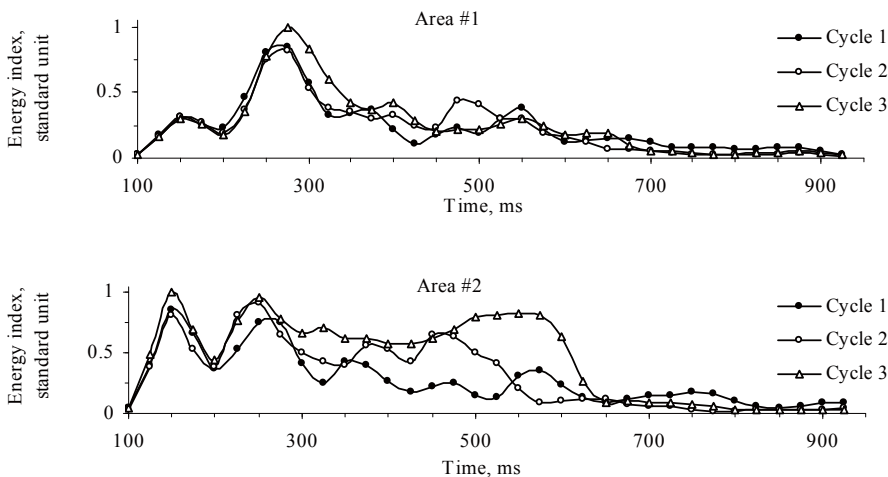


Figure 3. Seismic signals as absolute values of the amplitudes reduced by the energy index of the first signal phase with averaging the signal energy index in 50 ms time window and navigating the window based on the signal duration with 25 ms interval.

The difference of these signals by observation cycles enables us to identify three time bands: 100-160 ms, 300-450 ms and 500-950 ms. The first time band is typical for refracted waves (which propagation velocity is 400-500 m/s), the second one – for surface waves (150-200 m/s), and the third one – for low-velocity low-frequency waves (70-120 m/s). Energy index of the signals for three observation cycles based on the mentioned time bands is shown in Figure 4.

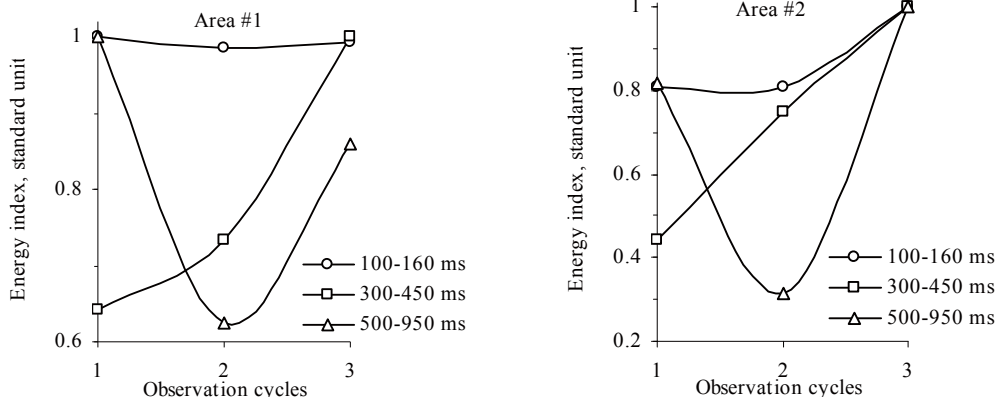


Figure 4. The energy index of seismic signals of different time bands based on three observation cycles.

The second time band is characterized by highly apparent increase in the energy index of the waves from cycles 1-2 and 3. At the area #1 this index increases by half, and at the area #2 it increases two-fold. During monitoring there was no precipitation that influences the propagation of surface waves. Therefore, taking into consideration location of the areas with regard to the active overlap fault and subsidence profile being formed, the reason of the changes in the waves under examination is the redistribution of stress state of rock mass.

The third time band differs by the character and magnitude of changes in the energy index of the waves with time. This index decreases at first (from cycle 1 to cycle 2) and then increases (from cycle 2 to

We can see that in the first time band (100-160 ms) the energy index practically does not change, or, as at the area #2, changes a little (up to 20%). Therefore refracted waves within their basic frequency (of the order of 30 Hz) shall be considered as the less sensitive of the analyzed wave types. The reason for this is apparently the long wavelength at this frequency (about 15 m) at which the sensitivity of refracted waves is much lower than that of the examined high-frequency components of these waves.

cycle 3). Its value changes two-threefold. Such large range of changes in the energy index speaks for high sensitivity of low-velocity low-frequency waves. High sensitivity of these waves is specified by the characteristics of their propagation in conditions of the original seismic channel. The upper boundary of the channel is ground surface; the lower boundary is top of rocks with increased elastic parameters. In this case a seismic wave is generated as a result of sequential reflection of signals from the above boundaries at the angle near to 90° at which elastic waves undergo small refraction. Due to such path waves pass a distance that exceeds the sounding base (source point interval/spacing) by many times and accumulate the impact of the stress state of rock mass.

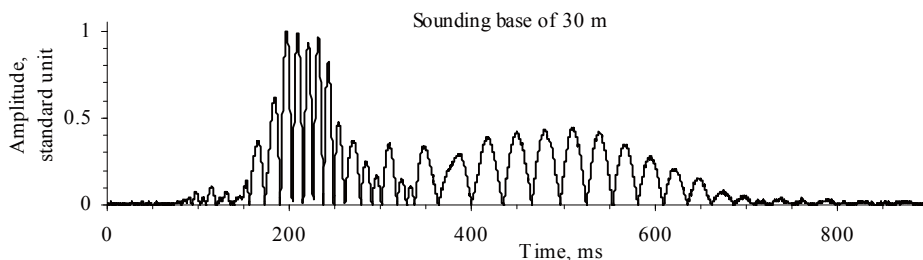


Figure 5. Low-velocity low-frequency wavetrain in the time band of 400-600 ms at seismic records obtained based on the different sounding bases.

Low-velocity low-frequency waves as a low-frequency wavetrain (11-18 Hz) are notably traced at seismic records obtained at the sounding bases of 30 and 60 m (Figure 5).

Amplitude levels of these waves in regard to the surface and refracted waves with the increase in the sounding base practically do not change. This feature shows that low-velocity low-frequency waves propagate in the seismic channel. In favor of their channel nature speaks also comparatively narrow spectrum and existence of dispersion (Figure 6).

Hence, taking into account the mode of propagation and significant changes in the energy index we

can consider the low-frequency waves as the most sensitive indicator of the changes in stress state of rock mass.

It should also be stated that in spite of different nature of their generation the refracted and low-velocity low-frequency waves are characterized by correlation of energy indices changing with observation time (see Figure 2 and 4). This fact speaks for physical objectivity of the employed energy index as well as the capability of using the high-frequency components of refracted waves and low-velocity low-frequency waves for reliable estimation of the changes in the stress state of rock mass.

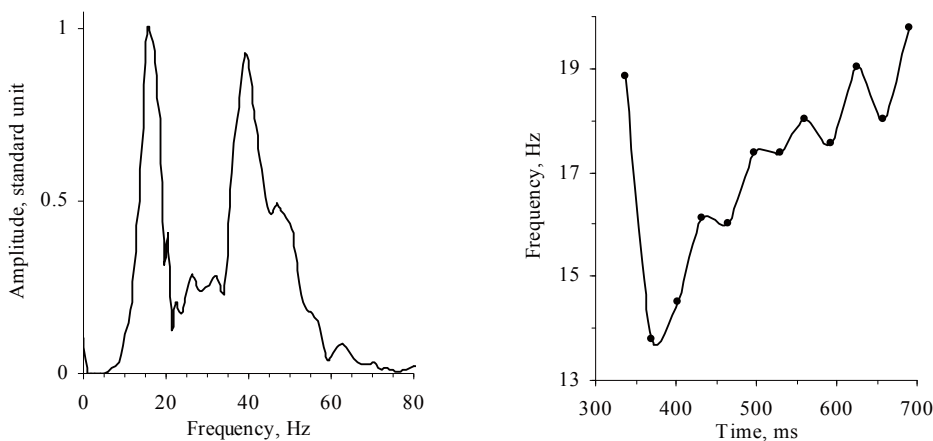


Figure 6. Seismic spectrum and frequency-wavetrain duration function for low-velocity low-frequency waves obtained at the sounding base of 30 m.

Thus, the outcomes of the survey are as follows.

1. Seismic sounding down to the overburden depth enables to detect redistribution of the stress state due to undermining of coal-rock mass and recent fault movements.

2. Due to the redistribution of the stress state the energy indicator of low-velocity low-frequency waves of channel nature can increase and decrease two-threefold and the energy indicator of high-frequency component of the refracted waves can change by a factor of four.

3. Low-velocity low-frequency waves of channel nature and high-frequency component of the refracted waves can be used for verifiable and operating control of the current changes in the stress state of coal-rock mass.

## REFERENCES

Antsyferov, A. V., Tirkel, M.G., Glukhov, A.A., Trifonov, A.S. & Tumanov, V.V. 2009. *Development of the fun-*

*damentals of seismic monitoring of geomechanical state of rock mass when working coal deposits of Ukraine.* Methods and Systems of seismodeformation monitoring of induces earthquakes and rock bursts. Novosybirsk: Mining Institute of the Siberian Branch of the RAS.

Trifonov, A.S., Kiselev, N.N., Tumanov, V.V., Buzhdezhan, A.V. Khlyustov, N.V. & Yalputa, Ye.A. 2012. *Manifestations of human-induced faulting of rock mass in energy indices of seismic waves.* Donetsk: Transactions of UkrSRMI of the NAS of Ukraine: Collection of Scientific Papers, 11: 267-274.

Trifonov, A.S., Arkhipenko, A.I., Khlyustov, N.V. & Yalputa, Ye.A. 2010. *Seismic surveys of geomechanical state of the overburden in active development of exogenous geological processes.* Donetsk: Transactions of UkrSRMI of the NAS of Ukraine: Collection of Scientific Papers, 6: 294-300.

Antsyferov, A.V., Trifonov, A.S., Tirkel, M.G., Tumanov, V.V. 2009. *Estimation of the stress state of the undermined rock mass based on the parameters of seismic reflections.* Donetsk: Transactions of UkrSRMI of the NAS of Ukraine: Collection of Scientific Papers, 5 (Part 1): 434-440.

Trifonov, A.S., Tirkel, M.G., Tumanov V.V. & Arkhipenko A.I. 2009. *Research into the impact of stress state of the*

*upper part of the rock mass being undermined on seismic signals parameters.* Donetsk: Transactions of UkrSRMI of the NAS of Ukraine: Collection of Scientific Papers, 4: 61-70.

Antsyferov, A. V., Tirkel, M.G., Trifonov, A.S. & Tumanov, V.V. 2008. *Seismic monitoring of coal-rock mass above production workings.* Proceedings of the Conference *Fundamental problems of formation of technogenic*

*geoenvironment.* Mining Institute of the RAS. Novosybirsk.

Antsyferov, A. V., Tirkel, M.G., Trifonov, A.S. & Tumanov, V.V. 2007. *Diagnostic seismic monitoring geodynamic state of the rock mass when mining coal seams.* Proceedings of the Conference *Geodynamics and Stress State of Subsurface.* Mining Institute of the RAS. Novosybirsk.



# Taylor & Francis

Taylor & Francis Group

<http://taylorandfrancis.com>